

See discussions, stats, and author profiles for this publication at: <https://www.researchgate.net/publication/230754970>

Mitochondrial ADP/ATP Carrier: Preventing Conformational Changes by Point Mutations Inactivates Nucleotide Transport Activity

ARTICLE *in* BIOCHEMISTRY · AUGUST 2012

Impact Factor: 3.02 · DOI: 10.1021/bi300978z · Source: PubMed

CITATIONS

2

READS

23

5 AUTHORS, INCLUDING:



[Marion Babot](#)

University of Dundee

11 PUBLICATIONS 71 CITATIONS

SEE PROFILE



[Guy Jean-Marie Lauquin](#)

French National Centre for Scientific Research

107 PUBLICATIONS 3,127 CITATIONS

SEE PROFILE

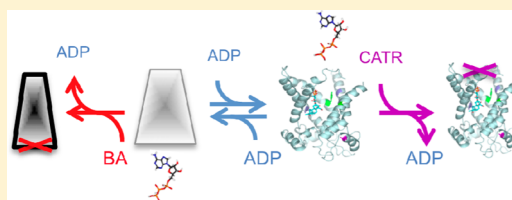
Mitochondrial ADP/ATP Carrier: Preventing Conformational Changes by Point Mutations Inactivates Nucleotide Transport Activity

Marion Babet,^{§,†} Corinne Blancard,[§] Igor Zeman,[‡] Guy J.-M. Lauquin,[§] and Véronique Trézéguet^{*,§,‡}

[§]Laboratoire de Physiologie Moléculaire et Cellulaire, Univ. de Bordeaux, IBGC, UMR 5095, F-33000 Bordeaux, France, and CNRS, IBGC, UMR 5095, F-33000 Bordeaux, France

[‡]Department of Biochemistry, Faculty of Natural Sciences, Comenius University, Mlynska dolina CH-1, 842 15 Bratislava, Slovakia

ABSTRACT: The mitochondrial ADP/ATP carrier (Ancp) is a paradigm of the mitochondrial carrier family (MCF); its members allow metabolic fluxes between mitochondria and the cytosol. The members of the MCF share numerous structural and functional characteristics. Ancp is very specifically inhibited by two classes of compounds, which stabilize the carrier in two different conformations involved in nucleotide transport. Resolution of the atomic structure of the bovine Ancp, in complex with one of its specific inhibitors, is that of the carrier open toward the intermembrane space. To gain insights into the interconversion from one conformation to the other, we introduced point mutations in the yeast carrier at positions Cys73 in the first matrix loop and Tyr97 and Gly298 in transmembrane helices 2 and 6. We demonstrate in this paper that they impair stabilization of the carrier in one conformation or the other, resulting in an almost complete inactivation of nucleotide transport in both cases. The results are discussed on the basis of the atomic structure of the conformation open to the cytosol. These mutant proteins could afford convenient tools for undertaking structural studies of both conformations of the yeast carrier.



In a eukaryotic cell, the members of the mitochondrial carrier family (MCF) allow fluxes of various metabolites between the cytosol and mitochondria. They share numerous structural and functional characteristics, and the mitochondrial ADP/ATP carrier (Ancp) is considered their paradigm and is the most abundant of them, except in brown adipose tissue where uncoupling protein 1 (UCP1) is the major carrier protein. Ancp is a key gate between mitochondria, where ATP is produced, and the cytosol, where ATP is consumed in cellular processes. Indeed, it provides the mitochondrial ATP synthase with one of its substrates, ADP or ATP depending on the physiological conditions, and as such is responsible for the specificity of nucleotide diphosphate phosphorylation in mitochondria. Ancp has to cope with high nucleotide fluxes to fulfill cell energetic requirements. Ancp is a protein of ~300 amino acids, located within the mitochondrial inner membrane (MIM) and catalyzes the exchange of one ADP³⁻ for one ATP⁴⁻. There is no net uptake of ADP or ATP, and Ancp uses the membrane potential generated by the respiratory chain to promote ADP³⁻ entry rather than ATP⁴⁻ entry. An ADP/ATP exchange between mitochondria and the cytosol was first described in the early 1960s. The discovery of two classes of very specific and powerful inhibitors, ATR (and CATR) and BA (and isoBA), allowed 40 years of extensive cellular, mitochondrial, and molecular studies. It was thus demonstrated that each class specifically binds to two different conformations of Ancp and stabilizes Ancp in what is now called the “CATR” conformation (ATR or CATR binding) and the “BA” conformation (BA or isoBA binding), which exhibit different reactivities toward chemical reagents or proteases, and different intrinsic fluorescence properties.^{1–3} To precisely decipher the nucleo-

tide transport mechanism, it is necessary to delineate the Ancp conformational changes inherent to the transport and therefore to gain deeper insights into the different conformational states of Ancp. Indeed, membrane transporters are characterized by their ability to swing from one conformation, which roughly exposes a hydrophilic cavity of the transporter toward one side of the membrane, to another conformation, which exposes a cavity toward the other side of the membrane.

In 2003, the atomic structure of beef Ancp (BtAnc1p) in complex with CATR was determined at high resolution.⁴ In this structure, the cavity is open toward the intermembrane space and CATR lies deep inside. The six tilted transmembrane segments of BtAnc1p (TMH1–6) delineate this cavity. Though this was a real breakthrough, essential questions about the precise nucleotide exchange mechanism, which involves interconversion between the BA and CATR conformations, remain unanswered. At this point, the atomic structure of the BA conformation is sorely lacking. Numerous attempts were made to purify the BtAnc1p in complex with BA. It appeared that, because of the chemical properties of BA, purification of Ancp in complex with BA is very improbable (G. Brandolin, personal communication). In this context, an Ancp mutant stabilized in the BA conformation could help solve this problem. The yeast *Saccharomyces cerevisiae* ScAnc2p affords a very convenient tool because its gene can be easily mutagenized. Three nuclear genes encode ScAncp, but only

Received: July 20, 2012

Revised: August 27, 2012

Published: August 28, 2012



ScANC2 is required for growth on nonfermentable carbon sources.^{5–8} A three-dimensional (3D) model of ScAnc2p in the CATR conformation was built from the BtAnc1p crystal structure because the amino acid sequences of both proteins are 47% identical. This allowed the rationalization of mutagenesis sites to unravel the nucleotide-binding site and pathway during nucleotide transport.⁹ However, the atomic structure corresponding to Protein Data Bank (PDB) entry 1okc was recently refined, and a new model was constructed, taking into account the recently determined structure of ATR (Figure 1).¹⁰ Though

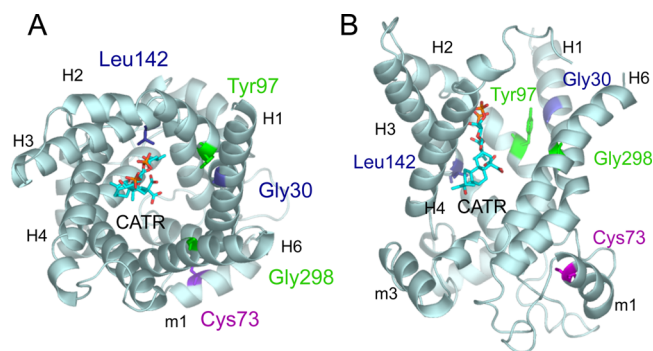


Figure 1. Modeling of the ScAnc2p 3D structure in complex with CATR. Ribbon representation for the protein and sticks for the indicated residues and CATR. A 3D model of Anc2p from *S. cerevisiae* based on the template structure of BtAnc1p was constructed with SWISS-MODEL using a specific template (automatic modeling mode).¹⁰ The ScAnc2p model was built using PHENIX. The carboxyatractyloside ligand was positioned as in the refined structure of BtAnc1p. The four mutated residues that confer BA resistance are colored dark blue (Gly30 and Leu142) or light green (Tyr97 and Gly298). The Cys73 residue is colored pink. In the refined structure of BtAnc1p, Leu127, which corresponds to Leu142 of ScAnc2p, is in van der Waals contact with the isovaleric group of CATR. The carboxylate that is specific to CATR forms a salt bridge with Arg79, which corresponds to Arg96 in ScAnc2p. CATR is carboxyatractyloside. (A) View from the intermembrane space, parallel to the plane of the membrane. H1–H6 correspond to TMH1–6, respectively, and m1 and m3 correspond to matrix loops m1 and m3, respectively. (B) View perpendicular to the plane of the membrane. TMH5 (H5) was omitted for the sake of clarity.

the two proteins are significantly similar, they exhibit biochemical properties different enough to suggest that their atomic structures could differ at some points. Therefore, we designed two ScAnc2p mutants (Tyr97Cys/Gly298Ser and Cys73Trp) stabilized in the CATR and the BA conformations. The rationale of our approach was to delineate more precisely the regions involved in the conformational changes and to facilitate further structural studies. Indeed, we aim to purify ScAnc2p without adding inhibitors, which as already mentioned proved to be particularly arduous in the case of the BA conformation.

We show in this paper that yeast cells expressing either of the two ScAnc2p variants are unable to grow on a nonfermentable carbon source, indicating Ancp and mitochondrial dysfunction. ATR binding as well as ADP/ATP exchange capabilities are studied to characterize further the consequences of these mutations.

To investigate the ability of ScAnc2p^{Tyr97Cys/Gly298Ser} and ScAnc2p^{Cys73Trp} to undergo conformational changes in the presence or absence of ligands, we used the “conformation reporter”, Val176Cys, which was developed in a previous work.⁹

We demonstrate that ScAnc2p^{Tyr97Cys/Gly298Ser} is stabilized in a CATR-like conformation and ScAnc2p^{Cys73Trp} in a BA-like conformation. As already mentioned, one of the aims of this study is to show that ScAnc2p point mutants can afford very convenient tools for structural studies if they avoid the use of inhibitors. Therefore, ScAnc2p^{Tyr97Cys/Gly298Ser} was tagged with a cluster of histidines, purified by affinity chromatography, and submitted to crystallization trials.

MATERIALS AND METHODS

Chemicals. [³H]Atractyloside ([³H]ATR) and 3′-O-(1-naphthoyl)adenosine 5′-diphosphate (N-ADP) were synthesized as previously described.^{11,12} The protein concentration was determined using the bicinchoninic acid reagent kit from Sigma. Nucleotides and CATR were purchased from Sigma, and P₁P₅-di(adenosine-5′)-pentaphosphate was from Calbiochem. The hexokinase/glucose-6-phosphate dehydrogenase enzyme mix was obtained from Roche Diagnostics GmbH.

Strains, Media, and Transformation. The XL1-Blue {recA1 endA1 gyrA96 (Nal^r) thi hsdR17 (r_K[−] m_K⁺) supE44 relA1 lac[−] F′ [Tn10 (tet^r) proAB⁺ lacI^q lacZΔM15]} *Escherichia coli* strain was used for plasmid propagation. The *JL1Δ2Δ3u*− (MATα leu2–3,112 his3–11,15 ade2–1 trp1–1 ura3–1 can1–100 anc1::LEU2 Δanc2::HIS3 Δanc3::ura3[−]) *S. cerevisiae* strain was used in this study.⁹

Yeast and bacteria cultivations and transformations and the composition of all the media used (YPD, YPLact, and SGal-Trp) have been described by De Marcos Lousa et al.¹³

Site-Directed Mutagenesis. Site-directed mutagenesis of ScANC2 was performed by polymerase chain reaction or with the Transformer Site-directed Mutagenesis Kit (CLONTECH Laboratories) using the following mutagenic primers (mutated bases are underlined, and the amino acid substitution is in parentheses): ²⁰⁶5′-GTATCTTAGACTGGTTC AAGA-GAACCGC-3′²³³ (Cys73Trp), ²³³5′-GCGGTTCTCTTGAAC-CAGTCTAAGATAC-3′²⁰⁶ (Cys73Trp reverse), ²⁷⁷5′-AACGT-TATCCGTTGTTTCCCCACTCAAGC-3′³⁰⁵ (Tyr97Cys), ³⁰⁵5′-GCTTGAGTGGGGAAACAACGGATAACGTT-3′²⁷⁷ (Tyr97Cys reverse), ⁸⁷⁰5′-TAAGAGGTGTCTG-CAAGTGCTGGTGTATCTC-3′⁹⁰⁸ (Gly298Ser), and ⁹⁰⁸5′-GAGATAACACCAGCACTTGCGACACCTCTTA-3′⁸⁷⁰ (Gly298Ser reverse).

The wild-type and mutated ScANC2 genes were subcloned into a centromeric plasmid, pRS314, under the control of the ScANC2 regulatory sequences as previously described.⁹ The resulting plasmids were used to transform the *JL1Δ2Δ3u*− strain to assess their ability to complement the *scanc2* deletion.

Preparation of Yeast Cell Extracts and Immunostaining. Cell proteins were extracted by the postalcaline method described by Kushnirov.¹⁴ Briefly, cells were grown in SGal-Trp medium until their A₆₀₀ reached 2–3. Cells were harvested and resuspended in 100 μL of 0.2 M NaOH. After 5 min at room temperature and a rapid centrifugation, the pellet was resuspended in 10 mM Tris-HCl (pH 6.8), 5% glycerol, 2% SDS, 4% β-mercaptoethanol, and 0.0025% bromophenol blue. It was boiled for 3 min, and 6 μL of the supernatant was loaded on a 12.5% SDS–PAGE gel. Tubulin was detected after the sample had been transferred onto a nitrocellulose membrane with an anti-tubulin antibody (1/2000) kindly provided by A. Baines.¹⁵

Isolation of Mitochondria, Immunostaining, Kinetic Measurements, and EMA Labeling. Yeast cells used for the isolation of mitochondria were grown in minimal synthetic

medium consisting of 0.17% yeast nitrogen base with or without amino acids and ammonium sulfate, 0.5% $(\text{NH}_4)_2\text{SO}_4$, 2% galactose, and all amino acids except tryptophan (SGal-Trp) to allow the plasmid to be maintained in the transformants. The protocols and materials used to perform isolation of mitochondria, ADP/ATP transport, $[\text{^3H}]$ ATR binding measurements, and protein immunostaining have been described by Babot et al.¹⁶ Briefly, freshly isolated mitochondria were incubated in the presence of an energy-generating system, an ATP detection enzymatic system based on NADP reduction, and variable concentrations of free ADP. The exchange was followed at 340 nm. Various $[\text{^3H}]$ ATR concentrations were incubated with isolated mitochondria (1 mg). After incubation on ice (45 min), mitochondria were pelleted, washed, and lysed with 5% Triton X-100 and 0.5 M NaCl. Radioactivity associated with the pellet was used to determine the amount of $[\text{^3H}]$ ATR bound to mitochondria. Nonspecific binding was assessed in the presence of 500 μM CATR. For protein immunostaining, mitochondria were isolated from cells grown in SGal-Trp. After the sample had been transferred, the nitrocellulose membrane was then immunodecorated with an antibody raised against ScAnc2p (1/14000) and an antibody raised against yeast α -tubulin (1/2000) or yeast porin (1/14000) for the cell or mitochondrial protein extract, respectively.^{15,17,18} After ECL detection with a GENE GNOME system (Syngene, Ozyme), signal intensities of the bands were quantified with ImageJ.¹⁶ The time course of the CATR-induced release of bound 3'-O-(1-naphthoyl)-adenosine 5'-diphosphate (N-ADP) binding was studied as described previously.¹³ Briefly, the fluorescence level was set to zero. Addition of CATR released N-ADP from mitochondria, inducing an increase in fluorescence (ΔF). The $K_{1/2}$ value was determined by plotting $\Delta F/\Delta F_{\text{max}}$ as a function of added N-ADP. EMA labeling of membrane-embedded ScAnc2p variants has been described by David et al.⁹

Construction and Purification of His-Tagged ScAnc2p^{Tyr97Cys/Gly298Ser}. ScAnc2p^{Tyr97Cys/Gly298Ser} was tagged with nine histidines and purified by affinity chromatography as described for wild-type ScAnc2p.¹⁹ Briefly, the carrier is purified after solubilization of isolated mitochondria with 3% *n*-dodecyl β -D-maltoside (DDM). The lysate is supplemented with 2 mM magnesium chloride and 20 mM imidazole and loaded onto the equilibrated Ni-NTA resin using a batch procedure. After the sample has been extensively washed, the carrier is eluted with 3 resin volumes of a buffer containing 500 mM imidazole. Elution of the protein is followed by the measurement of absorbance at 280 nm.

Imidazole is removed by Ultrogel AcA 202 size exclusion chromatography. The fraction of interest is loaded on Amicon Centriprep YM30 units (Millipore, molecular mass cutoff of 30000 Da) to reduce 10-fold the fraction volume. The detergent is concentrated at the same time, and this may lead to protein denaturation. Thus, it is removed using SM2 Bio-Beads after each round of concentration to reach a final concentration of 5–8 mg of protein/mL in 0.05% DDM.¹⁹

Construction of a Three-Dimensional Model Structure for ScAnc2p. A three-dimensional model of ScAnc2p was built on the basis of the refined template structure of BtAnc1p with SWISS-MODEL using a specific template (automatic modeling mode).^{10,20} The full model was regularized by molecular dynamics and simulated annealing, using the standard protocols implemented with Phenix.²¹

Crystallization Trials and Crystal Analyses. The first crystallization trials were conducted by vapor diffusion techniques with different commercial screens, using 96-well crystallization plates with sitting drops, and incubation at 20 °C. Protein drops (0.3 μL) were mixed with an equal volume of reservoir solution and equilibrated versus 100 μL of reservoir solution.

Data were collected at 100 K using synchrotron radiation on beamline ID23-2 at the ESRF (European Synchrotron Radiation Facility, Grenoble, France).

RESULTS

The Cys73Trp Mutation Is Deleterious to Yeast Growth and ADP/ATP Exchange Activity. To design a ScAnc2p mutant that would be stabilized in the BA conformation, we found the cysteinyl residue in position 73 (Cys73) in the middle of m1 (Figure 1) to be of interest. Indeed, labeling of the corresponding residue of BtAnc1p, Cys56, with *N*-ethylmaleimide (NEM) inhibited nucleotide transport by BtAnc1p.²² The reactivity of Cys56 to NEM induced by ADP or ATP was inhibited by CATR or ATR but not by BA. These results are in line with the accessibility of loop m1 to proteases in the BA conformation but not in the CATR conformation.²³ Because NEM added to isolated beef mitochondria inhibited ATR or CATR binding but not BA binding, it was hypothesized that covalently bound NEM trapped the carrier in the BA conformation.^{24,25} In the 3D structure of the BtAnc1p–CATR complex, Cys56 is buried inside the carrier (Figure 1). As a consequence, introducing a bulky residue (NEM) at this position would prevent stabilization of the protein in a CATR-like conformation. Cys56 of BtAncp is conserved in almost all forms of Ancp (92%) and corresponds to Cys73 in ScAnc2p. Mutation of Cys73 to Ser or Ala in ScAnc2p showed that this residue is not essential to transport activity.^{26–28} Therefore, we mutated Cys73 of ScAnc2p to Trp, which is a bulky residue mimicking the steric hindrance contributed by NEM labeling. We expected that this mutation would inhibit ATR binding and nucleotide exchange and would enhance the probability of the BA conformer because NEM labeling of Cys56 of BtAnc1p traps the carrier in the BA conformation.²²

JL1Δ2Δ3u[−] cells were transformed with the ScAnc2p^{Cys73Trp} mutant, and growth properties were evaluated in the presence of a fermentable carbon source (glucose, Sc-Trp) or a nonfermentable one (lactate, YPLact), in which case an intact mitochondrial function is required for growth. Indeed, the *JL1Δ2Δ3u[−]* strain is deleted for its endogenous ANC genes and can still grow in the presence of glucose but not in the presence of lactate. Therefore, this strain allows easy evaluation of whether a ScAnc2p mutant is active (growth on lactate) or not (no growth on lactate). As seen in Figure 2, the cells transformed with the Cys73Trp variant barely grew on lactate. In liquid culture, the doubling time was increased 8.5 times compared to that of the wild type (Table 1) with a growth yield value of 8, compared to 12 for the wild type, indicating the ScAnc2p^{Cys73Trp} mutant was not completely inactive. Therefore, in the following, cells were grown in minimal medium with all amino acids but tryptophan (for plasmid maintenance) and containing galactose as a fermentable carbon source (SGal-Trp).

Next, we estimated the relative ScAnc2p content in whole cells and in mitochondria from immunostaining experiments. Different amounts of mitochondrial proteins were subjected to

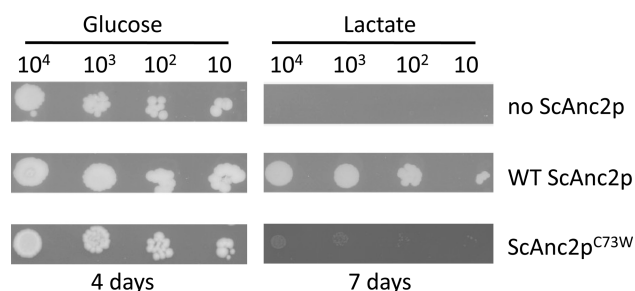


Figure 2. Deleterious effect of Cys73Trp mutation on yeast growth in the presence of lactate *JL1Δ2Δ3u⁻* transformed with the pRS314 plasmid containing no insert (no Ancp) or the gene encoding wild-type ScAnc2p (WT) or the ScAnc2p^{Cys73Trp} variant. Transformants were cultivated at 28 °C for 4 days on SC-Trp minimal medium (Glucose) or 7 days on lactate-containing rich medium (Lactate).

SDS–PAGE. After transfer, the nitrocellulose membrane was immunostained with an antibody raised against ScAnc2p and an antibody raised against yeast porin or α -tubulin. Intensities of the signals were quantified, and the ScAnc2p/tubulin (cell extracts) or ScAnc2p/porin (mitochondrial extracts) ratios in arbitrary units were set to 1 for the WT protein. The amount of the ScAnc2p^{Cys73Trp} variant represented $74 \pm 2\%$ of the WT protein in cells or $79 \pm 9\%$ in mitochondria (Table 1), indicating the Cys73Trp mutation did not prevent the insertion of ScAnc2p into mitochondria.

This variant was further characterized at a molecular level, by measuring the ADP/ATP exchange parameters on isolated mitochondria. As presented in Table 2, the K_m value for external ADP is increased 2.3 times and the V_{max} value is decreased 8.7 times. As a consequence, the V_{max}/K_m ratio, which reflects the mitochondrial efficiency, is decreased 20 times, indicating a very low efficiency at low nucleotide concentrations, in spite of an almost normal amount of Ancp in mitochondria, as measured by immunostaining (Table 1). This can account for the poor growth of the Cys73Trp strain observed in the presence of lactate.

The low ADP/ATP transport efficiency could arise from the inability of ScAnc2p^{Cys73Trp} to either bind nucleotides or undergo the conformational changes necessary for nucleotide transport. We first investigated ADP binding through the use of N-ADP. N-ADP is a nontransportable fluorescent ADP analogue, and its binding to Ancp can be examined with isolated mitochondria.²⁹ Its fluorescence is quenched upon binding to Ancp, so specific binding can be measured by the fluorescence enhancement observed upon dissociation after the addition of CATR. The $K_{1/2}$ value for binding of N-ADP to

WT ScAnc2p is $1.1 \pm 0.2 \mu\text{M}$ and 3.1 times higher for ScAnc2p^{Cys73Trp} (Table 2). However, the maximal N-ADP binding is only 50% of that obtained with WT ScAnc2p (data not shown). This could be due to either poor N-ADP binding (although this hypothesis does not fit with the $K_{1/2}^{\text{N-ADP}}$ value and the K_m^{ADP} value obtained for nucleotide exchange) or poor CATR binding, which, upon addition, releases bound N-ADP. Therefore, we performed [³H]ATR binding experiments on mitochondria isolated from the strain producing ScAnc2p^{Cys73Trp}. This binding was unmeasurable, regardless of the concentration of added [³H]ATR, up to $6 \mu\text{M}$. Though CATR can release part of the bound N-ADP, it appears from these experiments that ScAnc2p^{Cys73Trp} cannot bind ATR or cannot form a stable complex with ATR, and probably only with difficulty with CATR. This reinforces our hypothesis of ScAnc2p^{Cys73Trp} adopting preferentially the BA conformation and being unable to swing stably to the CATR one, which is mandatory for ADP/ATP transport. [³H]ATR binding experiments measure the amount of presumably properly folded ScAnc2p in mitochondria. Indeed, ATR binds to an Ancp conformation involved in nucleotide exchange, and we assume that a ScAnc2p mutant preferentially stabilized in the BA conformation will bind the other class of inhibitors, ATR and CATR, with difficulty (see Discussion).

Combining Tyr97Cys and Gly298Ser Mutations Does Not Prevent ADP Binding but Impairs ADP/ATP Exchange Activity. To design a mutant preferentially stabilized in the CATR conformation, we hypothesized that such a mutant would barely respond to BA. We previously identified four ScAnc2p amino acids that, when mutated, led to yeast cell resistance to BA: Gly30Ser, Tyr97Cys, Leu142Tyr, and Gly298Ser (Figure 1).³⁰ All these residues are located in transmembrane segments (TMH1–4, respectively) approximately in the center of the cavity open to the intermembrane space (IMS). They are very well conserved in all known Ancp sequences (100, 99, 95, and 97%, respectively). In the 3D structure of the bovine Anc1p (PDB entry 1okc), Leu127, which corresponds to Leu142 of ScAnc2p, is in van der Waals contact with the isovaleric group of CATR and the carboxylate that is not shared with ATR forms a salt bridge with Arg79, which corresponds to Arg96 in ScAnc2p, which itself is close to Tyr97.^{4,10} The in vivo BA resistance was correlated neither with highly modified amounts of ScAnc2p variants in mitochondria nor with impaired ADP/ATP exchange properties. However, though the mutants exhibited an ADP/ATP exchange resistant to BA, none of them had lost the ability to bind BA. Indeed, the loss of BA binding may possibly lead to the loss of function because ScAnc2p would be unable to efficiently operate the

Table 1. Growth Properties and Cellular and Mitochondrial ScAnc2p Content of the Variants

	growth on lactate ^a		relative ScAnc2p content ^b	
	doubling time (h)	growth yield (A_{600})	cellular ^b	mitochondrial
WT ScAnc2p	2	12	1	1
ScAnc2p ^{Cys73Trp}	17	8	0.74 ± 0.02	0.79 ± 0.09
ScAnc2p ^{Tyr97Cys/Gly298Ser}	6.5	3.7	1.325 ± 0.007	0.85 ± 0.11
H9Anc2p ^{Tyr97Cys/Gly298Ser}	6.5	3.2	1.13 ± 0.04	nd ^c

^a*JL1Δ2Δ3u⁻* was transformed with the pRS314 plasmid containing no insert (no Ancp) or the indicated ScAnc2p variant gene. Transformants were cultivated at 28 °C in rich lactate-containing medium, and A_{600} was measured every 4 h over a period of 120 h to determine doubling time and growth yield (A_{600} during the stationary phase of the cultures). ^bThe relative ScAnc2p content was determined after immunostaining of cell proteins. The ScAnc2p/tubulin or ScAnc2p/porin ratios in arbitrary units were set to 1 for the wild-type protein. Data are means of at least two experiments.

^cNot determined.

Table 2. Kinetic Parameters of the ScAnc2p Variants

	ADP/ATP exchange parameters ^a		N-ADP binding ^b	ATR binding ^c	
	V_{\max}^{ADP} (nmol min ⁻¹ mg ⁻¹)	$K_{\text{M}}^{\text{ADP}}$ (μM)	$K_{1/2}$ (μM)	B_{\max}^{ATR} (pmol/mg)	$K_{\text{d}}^{\text{ATR}}$ (μM)
WT ScAnc2p	87 ± 5	1.5 ± 0.2	1.1 ± 0.2	1010 ± 77	192 ± 25
ScAnc2p ^{Cys73Trp}	10 ± 1	3.4 ± 0.8	3.4 ± 1.2	NM ^d	NM ^d
ScAnc2p ^{Tyr97Cys/Gly298Ser}	12 ± 1	0.31 ± 0.09	6.2 ± 2.1	344 ± 11	89 ± 11

^aThe ADP/ATP exchange was followed at 340 nm with freshly isolated mitochondria. The given values are the means of three to six different experiments. ^bVarious concentrations of N-ADP were added to isolated mitochondria (0.5 mg/mL). ^cVarious [³H]ATR concentrations were incubated with isolated mitochondria (1 mg). B_{\max}^{ATR} is the maximal number of ATR binding sites. ^dNonmeasurable.

conformational changes necessary for nucleotide transport. Interestingly, the four mutants could also bind ATR, though the Leu142Ser variant exhibited a significantly reduced affinity.

We combined two of these mutations, Tyr97Cys and Gly298Ser, to obtain a variant that cannot bind BA or with very weak affinity. We have chosen these mutations because of the high degree of conservation of Tyr97 and Gly298 throughout Ancp amino acid sequences specifically, contrary to Gly30, which is conserved among all MCF members. Leu142 was not considered because it exhibits a reduced affinity toward CATR.

After 4 days at 28 °C, the double mutant ScAnc2p^{Tyr97Cys/Gly298Ser} has not allowed growth of *JL1Δ2Δ3u⁻* on a solid medium with a nonfermentable carbon source (Figure 3) unlike the parent mutants. The doubling time

WT, whereas the affinity was 2 times higher, indicating that this variant is properly folded but cannot be efficiently stabilized in the form of a complex with ATR. Interestingly, these results evidence that ScAnc2p^{Tyr97Cys/Gly298Ser} is stable in vivo. ScAnc2p^{Tyr97Cys/Gly298Ser} would preferentially adopt a conformation open toward the intermembrane space, i.e., a CATR-like one.

Because ATR is a competitive inhibitor of ADP for nucleotide transport, it was of interest to determine if the kinetic parameters of ADP binding were modified for ScAnc2p^{Tyr97Cys/Gly298Ser}. The properties of binding of N-ADP to Ancp were examined with isolated mitochondria. The $K_{1/2}$ value is 6.2 ± 2.1 μM, which is 6 times higher than the value determined for yeast ScAnc2p [$K_{1/2}$ = 1.1 ± 0.2 μM (Table 2)], indicating altered ADP binding. Therefore, the question of whether ScAnc2p^{Tyr97Cys/Gly298Ser} can perform nucleotide transport arises. We measured ADP/ATP exchange kinetic parameters with mitochondria isolated from the strains expressing ScAnc2p^{Tyr97Cys/Gly298Ser}. As can be seen in Table 2, the V_{\max} value is decreased approximately 7 times while the K_M^{ADP} value (0.31 ± 0.09 μM) accounts for an increased affinity for ADP. However, the exchange efficiency at low ADP concentration, which corresponds to the V_{\max}/K_M ratio, is low. Its value is 12.3 compared to 58 for the WT (calculated from data in Table 2), and this could explain the absence of yeast growth when an active ScAnc2p is needed, i.e., in the presence of lactate (Figure 3 and Table 1).

Though ScAnc2p^{Tyr97Cys/Gly298Ser} binds nucleotides and ATR, its nucleotide exchange activity is impaired. We can suppose that it cannot perform the conformational changes necessary for nucleotide transport or stabilization in the BA conformation upon substrate binding. We did not measure BA binding because these experiments were not decisive in the case of the parent mutants. Indeed, BA binds to mitochondrial membranes because of its chemical nature.³⁰ Furthermore, at high concentrations, BA accumulates in the mitochondrial matrix.³¹

ScAnc2p^{Cys73Trp} and ScAnc2p^{Tyr97Cys/Gly298Ser} Are Stabilized in Different Conformations. From our results, it seems that the mutants we have designed switch with difficulty from one conformation to the other, and this could explain why they are unable to restore *JL1Δ2Δ3u⁻* growth on lactate. To investigate this hypothesis, we took advantage of a reporter mutation, Val176Cys, which allows the assessment of matrix loop 2 (m2) conformational changes.⁹ Indeed, CATR and BA induce conformational changes similar to those involved in nucleotide translocation during which m2 plays an important role. We previously described the ScAnc2CLp^{Val176Cys} mutant, in which the four endogenous cysteinyl residues were mutated to Ala (Anc2CLp) and Val176 in matrix loop m2 was mutated to Cys. Its accessibility to the nonpermeant reagent eosin-5-maleimide (EMA) depends on the ligands bound to the carrier. When it is bound to BA, Val176Cys is accessible to EMA

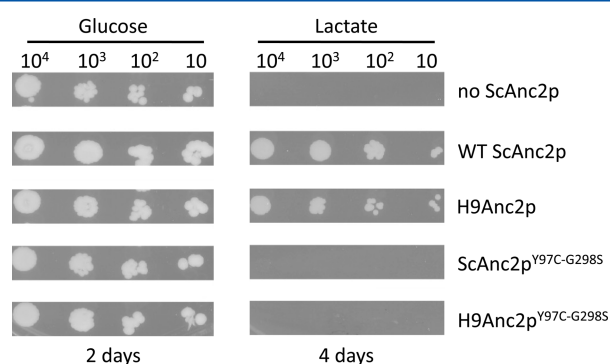


Figure 3. Combination of Tyr97Cys and Gly298Ser mutations has deleterious effect on yeast growth in the presence of lactate. *JL1Δ2Δ3u⁻* was transformed with the pRS314 plasmid containing no insert (no Ancp) or the gene encoding the indicated ScAnc2p variant: untagged or tagged wild type (WT or H9Anc2p) and untagged or tagged ScAnc2p^{Tyr97Cys/Gly298Ser} (ScAnc2p^{Tyr97Cys/Gly298Ser} or H9Anc2p^{Tyr97Cys/Gly298Ser}). Transformants were cultivated at 28 °C for 2 days on SC-Trp minimal medium (Glucose) or 4 days on lactate-containing rich medium (Lactate).

in liquid culture was increased to 6.5 h, as compared to 2 h for the wild type, and the biomass at growth saturation was dramatically reduced: 3.7 compared to 12 for the wild type (Table 1). We first controlled the conditions so that the growth deficiency did not arise from a synthesis defect of the mutant carrier. Yeast and mitochondrial extracts were prepared from cells grown in the presence of galactose, loaded onto an SDS-PAGE gel, and transferred onto a nitrocellulose membrane. As can be seen in Table 1, ScAnc2p^{Tyr97Cys/Gly298Ser} could be efficiently detected with an antibody raised against ScAnc2p and its cellular amount was even higher than that of WT ScAnc2p. [³H]ATR binding experiments (Table 2) showed that the maximal number of binding sites of ScAnc2p^{Tyr97Cys/Gly298Ser} was reduced to 34% of that of the

labeling, whereas when ScAnc2CLp^{Val176Cys} is in complex with CATR or ATR, Val176Cys is not accessible to EMA modification. Thus, Val176Cys EMA labeling appears to be a good reporter of ScAnc2p conformational changes induced by inhibitor binding.

This reporter mutation was introduced into ScAnc2p^{Cys73Trp} and ScAnc2p^{Tyr97Cys/Gly298Ser} to study their conformational changes upon ligand binding through EMA labeling performed with isolated mitochondria in the absence or presence of ADP, BA, or CATR. First, we checked that Cys97 was not labeled with EMA under these conditions (data not shown). As can be seen in Figure 4, whatever ligand was added,

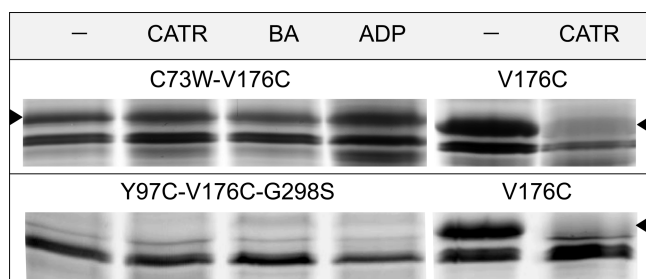


Figure 4. EMA labeling of Val176Cys in ScAnc2p^{Cys73Trp} and ScAnc2p^{Tyr97Cys/Gly298Ser}. Mitochondria were isolated from ScAnc2p^{Val176Cys} that had not been mutated (WT) or had been mutated (Cys73Trp or Tyr97Cys/Gly298Ser). Frozen–thawed mitochondria were incubated (8 mg of proteins/mL) with no ligand (none) or with 40 μ M CATR, 40 μ M BA, or 40 μ M ADP for 15 min on ice, as indicated. EMA labeling (400 μ M) was performed for 30 min on ice in the dark. The reaction was stopped with 20 mM DTT (10 min at 4 °C in the dark). Samples were subjected to SDS–PAGE, and fluorescence was visualized at 532 nm. The position of ScAnc2CLp^{Val176Cys}, indicated by an arrow, was controlled by immunostaining after the gel had been transferred onto a nitrocellulose membrane.

ScAnc2p^{Cys73Trp/Val176Cys} is always labeled while ScAnc2p^{Tyr97Cys/Gly298Ser/Val176Cys} is never labeled. In the case of ScAnc2p^{Tyr97Cys/Gly298Ser}, we have controlled the fact that the absence of labeling did not arise from limitation of EMA entry. For this purpose, labeling was performed with mitoplasts in which the outer mitochondrial membrane was disrupted. They were prepared by incubating isolated mitochondria in a hypoosmotic buffer. No EMA modification was observed under these conditions, though ScAnc2p^{Tyr97Cys/Gly298Ser/Val176Cys} was labeled when mitochondria were solubilized with Triton X-100 at a high concentration (3%, data not shown), which exposes most of ScAnc2p regions to the solvent and therefore to EMA. Our results suggest that ScAnc2p^{Cys73Trp} is preferentially stabilized in a BA-like conformation and ScAnc2p^{Tyr97Cys/Gly298Ser} in a CATR-like conformation. An alternative hypothesis is that both mutants can adopt only one conformation and cannot switch stably to the other (see Figure 5 and Discussion).

ScAnc2p^{Tyr97Cys/Gly298Ser} Is a Potential Candidate for Structural Studies. ScAnc2p^{Tyr97Cys/Gly298Ser} is stabilized in a CATR-like conformation and can still bind ADP and ATR. As it is produced in good quantity, it appears to be the right candidate for crystallization trials. To purify the protein, it was tagged with a set of nine histidines at its N-terminus and purified by affinity chromatography.¹⁹ Beforehand, we ensured that the histidine tag did not modify the *JL1Δ2Δ3u⁻* growth phenotype on lactate (Figure 3 and Table 1). The tagged

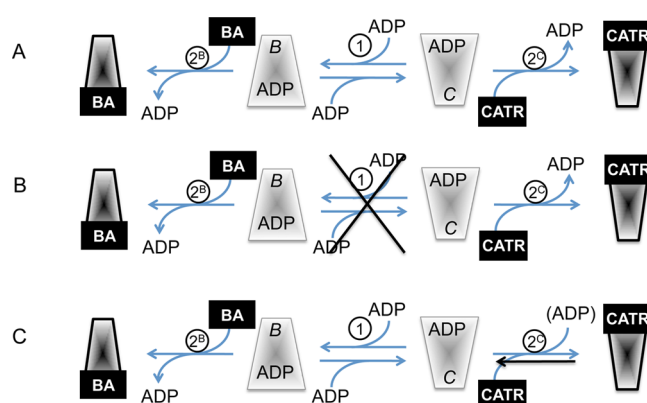


Figure 5. Model of the conformational changes undergone by Ancp during nucleotide transport. (A) Two different conformations (B for BA and C for CATR) exist in the membrane, and nucleotide binding (ADP) triggers their interconversion (step 1). Each conformation is stabilized by inhibitor binding: BA stabilizes the BA conformation (step 2^B) and CATR the C conformation (step 2^C). Steps 2^B and 2^C are considered irreversible. Either ScAnc2p^{Cys73Trp} cannot perform step 1 as depicted in panel B, or Step 2^B becomes reversible because of a very unstable Ancp–CATR complex, as depicted in panel C. ScAnc2p^{Tyr97Cys/Gly298Ser} either could not perform step 1 or would form a very unstable complex with BA.

variant, H9Anc2p^{Tyr97Cys/Gly298Ser}, was purified following the protocol described by Arnou et al.¹⁹ The carrier preparation was highly pure and unproteolyzed, as estimated by Coomassie Blue staining and immunostaining after SDS–PAGE (data not shown). After imidazole had been removed with an Ultrogel Aca 202 size exclusion chromatography column, the protein was concentrated ~10-fold. This step was followed by removal of excess detergent to avoid ScAnc2p denaturation (see Materials and Methods). Both steps were repeated until the H9ScAnc2p^{Tyr97Cys/Gly298Ser} concentration reached 5–8 mg/mL. It was immediately submitted to crystallization trials.

The crystallization trials were conducted by sitting-drop vapor diffusion techniques with different commercial screens, using 96-well crystallization plates, and incubation at 20 °C. Positive hits were mainly obtained for conditions containing PEG and buffers settled at pH 8.5. After 6 weeks, a round-shaped crystal was obtained with 0.2 M sodium citrate, 0.1 M Tris-HCl (pH 8.5), and 30% PEG 400. The presence of ScAnc2p in the crystal was assessed. After being washed with the reservoir solution, the crystal was dissolved in 2% SDS and spotted onto a nitrocellulose membrane. As a control, the drop in which the crystal appeared was submitted to a similar treatment. Immunostaining with anti-ScAnc2p antibodies revealed the presence of ScAnc2p in the crystal but not in the drop (data not shown). An X-ray diffraction analysis was performed on this crystal. Although the crystal diffracted in only two dimensions and at very low resolution (23 Å), data were tentatively indexed in space group *P1* with the following cell parameters: *a* = 47.6 Å, *b* = 48.3 Å, and *c* = 50.0 Å. For comparison, cell parameters of the bovine enzyme were as follows: *a* = 85.43 Å, *b* = 83.46 Å, *c* = 49.92 Å, and space group *P2₁2₁2₁*.⁴ The size of the molecule in the crystal is approximately 45 Å × 45 Å × 55 Å. Therefore, our results could account for a two-dimensional (2D) crystal of ScAnc2p.

DISCUSSION

Understanding the conformational changes undergone by Ancp is a central issue in deciphering the precise mechanism of ADP/ATP translocation across the mitochondrial inner membrane. The CATR conformation of BtAnc1p evidenced a large hydrophilic cavity open toward the intermembrane space and delineated by the six-tilted TMH of the carrier. CATR lies deeply inside and the cavity is closed on the matrix side. Wang et al. calculated the time-averaged electrostatic potential of BtAnc1p during a molecular dynamics simulation and found a strong positive potential of ~ 1.4 V at the entrance of the cavity.³² This high potential value could account for a rapid binding of ADP.³² Besides, site-directed mutagenesis of ScAnc2p evidenced the role of an aromatic ladder in TMH4 (Tyr203, Tyr207, Phe208, and Tyr211) in the transfer of ADP from one side of the carrier to the other. Tyr203 is involved in a stacking interaction with the diterpene moiety of CATR. Mutation of Tyr203 and Phe208 to alanines stabilized ScAnc2p in a CATR-like conformation and prevented interconversion to a BA-like conformation.⁹ At the bottom of the cavity, mutation of Met254 to alanine inactivated the carrier but could be compensated by second-site mutations, noticeably Gly30Cys, Tyr207His, and Gly298Ser.³³ As discussed in the introductory section, Gly30Ser and Gly298Ser mutations confer BA resistance to ScAnc2p. All of these results suggest that these two residues and Tyr207 of the aromatic ladder are involved in the interconversion of ScAnc2p from one conformation to the other. In this paper, we confirm the role of Gly298. Indeed, we demonstrate that the Tyr97Cys/Gly298Ser double mutant is locked in a CATR-like conformation. Tyr97 is next to Arg96, which is involved in a salt bridge with the carboxylic group of CATR not shared with ATR. Furthermore, mutation of Arg96 into histidine (*op1* mutation) inactivates ScAnc2p.⁷ This deleterious effect cannot be reversed by second-site mutation.³⁴ However, the Arg96His mutant efficiently binds ATR and ADP.³⁵ Furthermore, Arg79 of BtAnc1p (Arg96 of ScAnc2p) belongs to the basic patch, which along with the last residue of the aromatic ladder, Tyr186 of BtAnc2p (Tyr203 of ScAnc2p), constricts the cavity to 8 Å.⁴ It would be a site of attraction of the negative charges of the phosphate groups of ADP.^{32,36} Tyr97 and Gly298 are located on either side of TMH1, and Tyr97 is oriented toward TMH1. Any change in these residues could disrupt the relative arrangement of TMH1, -2, and -6, preventing, for example, reorganization of the salt bridge induced by nucleotide binding as hypothesized by Wang et al.³² The bond between Asp134 (Asp149) and Arg234 (Arg252) is disrupted, and a new one is established between Asp134 (Asp149) and Arg79 (Arg96).

EMA labeling of natural or engineered cysteines was used to decipher changes in ScAnc2p conformation upon ligand binding. The reactivity to EMA of residues 98–106 of transmembrane segment 2 (TMH2) mutated to cysteines varies depending on the presence of ATR or BA.³⁷ For example, Asn104 is labeled in the presence of CATR but not in the presence of BA. In the BtAnc1p structure, Asn87 (Asn104 of ScAnc2p) interacts with a sulfate group of CATR through hydrogen bonding, suggesting EMA can release ATR. Kihira et al. proposed a twisting of the middle part of TM2 (Gln101–Ala106) upon inhibitor binding that might be related to the conformational changes of matrix loop m1, induced upon inhibitor binding.³⁷

ScAnc2p exhibits inhibitor-dependent deuterium accessibility like BtAnc1p as seen through hydrogen/deuterium exchange experiments coupled to mass spectrometry.³³ However, in detergent solution, both proteins exhibit different conformational accessibilities. Namely, the upper part of the cavity is much less accessible to the solvent in the ScAnc2p–CATR complex than in the BtAnc1p–CATR complex.³⁸ The level of deuteration of BtAnc1p remains low in the presence of BA. While the three matrix loops (m1–m3) were protected in the BtAnc1p–CATR complex, only loop m2 was protected in the ScAnc2p–CATR complex. Furthermore, loop m2 of ScAnc2p can protrude into the membrane or the cavity.³ Therefore, in spite of their sequence similarities, ScAnc2p and BtAnc1p probably display different 3D structures, with a similar overall organization. It is thus a requisite to obtain the atomic structure of ScAnc2p in complex with its inhibitors to gain insights into the conformational changes undergone by ScAnc2p during ligand binding and nucleotide transport. For example, the instability of the carrier–BA complex in a detergent solution leads to a progressive release of BA. A mutant stabilized in a given conformation would afford a very convenient tool for undertaking structural studies, because it could be purified without the need of an inhibitor. To validate our assumption, it was preferable to investigate a mutant stabilized in the CATR conformation because it would be possible to compare the obtained data with the atomic structure of bovine Anc1p.⁴ ScAnc2p^{Tyr97Cys/Gly298Ser} was tagged with nine histidines at its N-terminus and purified with a high yield and high homogeneity. It was submitted to crystallization trials, and 2D crystals that diffracted at 23 Å resolution were obtained. Though this corresponds to a low resolution, this result is promising because the data could be indexed in space group *P1* with cell parameters compatible with what was observed with BtAnc1p.⁴ Other crystallization conditions are still under investigation.

Obtaining data about the BA conformation is much more challenging because of the chemical nature of BA, which can bind to the membranes and be dissociated from the protein in a detergent solution. Conformational changes of matrix loop m1 would be induced upon inhibitor binding and following twisting of TMH2.^{27,37} When Cys56 in the middle of loop m1 of BtAnc1p is labeled with NEM, it traps the carrier in a BA-like conformation.²⁴ Kihira et al. mutated Cys56 of BtAnc1p expressed in yeast to seven different amino acids.³⁹ Ala, Ser, Thr, or Val has no or little effect. However, no growth on a nonfermentable carbon source was observed with Gly, Asp, or Tyr. Though the corresponding variants were expressed and inserted into the MIM, none could sustain ADP uptake in isolated mitochondria. Similar mutations of the corresponding residue in ScAnc2p, Cys73, produced similar effects. However, the Cys73Ser mutant has an absolute requirement for cardiolipins during reconstitution experiments and therefore may be involved in cardiolipin interactions, which are part of the Ancp structure and, like for other MIM proteins, are necessary for their assembly in the MIM and/or their activity.^{27,40} We mimicked NEM labeling to trap the carrier in a BA-like conformation by mutating Cys73 to Trp. This mutation impaired ScAnc2p activity, and we demonstrate in this paper that this mutant cannot be stabilized by CATR or ATR and is stabilized in a BA-like conformation. This bulky residue probably precludes interaction of loop m1 with the membrane, occurring in the CATR conformation, leaving the protein open on the matrix side. Indeed, we can hypothesize that in the BA conformation, the hydrophilic cavity is close to

the intermembrane space and open to the matrix compartment. Matrix loops m1 and m3 of ScAnc2p are more accessible to the solvent than matrix loop m2 in the BA conformation.³³ They are probably folded out in the matrix, and rearrangement of the three loops allows the carrier to be open on the matrix side. This reorganization exposes the residues of the small hydrophilic helices that were buried in the CATR conformation, for example, Cys73, Val176, and Cys271 in matrix loops m1–m3, respectively.

In conclusion, we obtained two ScAnc2p mutants, by site-directed mutagenesis, which are stabilized in either of the two conformations involved in nucleotide transport. The mutations that favor the CATR conformation are located in the upper part of the hydrophilic cavity and could preclude closure of the cavity on the intermembrane space. The mutation that favors the BA conformation is located on the matrix side and possibly precludes closure of the carrier on the matrix side. Both mutants are stably produced, and preliminary structural experiments aimed at determining the atomic structure of ScAnc2p are promising and still being pursued.

AUTHOR INFORMATION

Corresponding Author

*Phone: (33) 5 4000 6847. Fax: (33) 5 4000 2200. E-mail: v.trezeguet@cbrmn.u-bordeaux.fr.

Present Addresses

[†]Queen's University Belfast, Medical Biology Centre, 97 Lisburn Rd., Belfast BT9 7BL, Northern Ireland.

[‡]CBMN UMR 5248, CNRS and Bordeaux University, Allée Geoffroy Saint-Hilaire, Bât B14b, 33600 Pessac, France.

Author Contributions

The manuscript was written through contributions of all authors. All authors have given approval to the final version of the manuscript.

Funding

This work was supported by the University of Bordeaux Segalen, the Centre National de la Recherche Scientifique, and the Région Aquitaine. M.B. was supported by the French Ministère de l'Enseignement Supérieur et de la Recherche.

Notes

The authors declare no competing financial interest.

ACKNOWLEDGMENTS

We thank the staff at the European Synchrotron Radiation Facilities and the French beamline ID23-2 (ESRF) for synchrotron support. We are grateful to Alain Dautant (IBGC, UMR5095) for X-ray diffraction analyses, Marie-France Giraud for her help in crystal mounting, Thierry Granier and Bernard Gallois for modeling the ScAnc2p structure from the refined structure of BtAnc1p, Emmanuel Tétaud (IBGC, UMR5095) for careful reading of the manuscript, and Amanda Birch for English editing.

ABBREVIATIONS

ANC, mitochondrial adenine nucleotide carrier (ADP/ATP carrier)-encoding gene; Ancp, adenine nucleotide carrier (ADP/ATP carrier); ATR, atractyloside; BtAnc1p, isoform 1 of *Bos taurus* Ancp; BA, bongkreikic acid; CATR, carboxyatractyloside; EMA, eosin-5-maleimide; Gal, galactose; IMS, inter membrane space; Lac, lactate; MCF, mitochondrial carrier family; MIM, mitochondrial inner membrane; N-ADP, 3'-O-(1-naphthoyl)adenosine 5'-diphosphate; NEM, N-ethylmaleimide;

Sc, *S. cerevisiae*; ScAnc2p, isoform 2 of *S. cerevisiae* Ancp; SDS-PAGE, sodium dodecyl sulfate–polyacrylamide gel electrophoresis; TMH, transmembrane helix; YPD, rich yeast extract peptone dextrose medium; WT, wild type.

REFERENCES

- (1) Brandolin, G., Le Saux, A., Trézéguet, V., Lauquin, G. J.-M., and Vignais, P. V. (1993) Chemical, immunological, enzymatic, and genetic approaches to studying the arrangement of the peptide chain of the ADP/ATP carrier in the mitochondrial membrane. *J. Bioenerg. Biomembr.* 25, 459–472.
- (2) Roux, P., Le Saux, A., Trézéguet, V., Fiore, C., Schwimmer, C., Dianoux, A. C., Vignais, P. V., Lauquin, G. J.-M., and Brandolin, G. (1996) Conformational changes of the yeast mitochondrial adenosine diphosphate/adenosine triphosphate carrier studied through its intrinsic fluorescence. 2. Assignment of tryptophanyl residues of the carrier to the responses to specific ligands. *Biochemistry* 35, 16125–16131.
- (3) Dahout-Gonzalez, C., Ramus, C., Dassa, E. P., Dianoux, A.-C., and Brandolin, G. (2005) Conformation-dependent swinging of the matrix loop m2 of the mitochondrial *Saccharomyces cerevisiae* ADP/ATP carrier. *Biochemistry* 44, 16310–16320.
- (4) Pebay-Peyroula, E., Dahout-Gonzalez, C., Kahn, R., Trézéguet, V., Lauquin, G. J.-M., and Brandolin, G. (2003) Structure of mitochondrial ADP/ATP carrier in complex with carboxyatractyloside. *Nature* 426, 39–44.
- (5) Adrian, G. S., McCammon, M. T., Montgomery, D. L., and Douglas, M. G. (1986) Sequences required for delivery and localization of the ADP/ATP translocator to the mitochondrial inner membrane. *Mol. Cell. Biol.* 6, 626–634.
- (6) Lawson, J. E., and Douglas, M. G. (1988) Separate genes encode functionally equivalent ADP/ATP carrier proteins in *Saccharomyces cerevisiae*. Isolation and analysis of AAC2. *J. Biol. Chem.* 263, 4812–4818.
- (7) Kolarov, J., Kolarova, N., and Nelson, N. (1990) A third ADP/ATP translocator gene in yeast. *J. Biol. Chem.* 265, 12711–12716.
- (8) O'Malley, K., Pratt, P., Robertson, J., Lilly, M., and Douglas, M. G. (1982) Selection of the nuclear gene for the mitochondrial adenine nucleotide translocator by genetic complementation of the *op1* mutation in yeast. *J. Biol. Chem.* 257, 2097–2103.
- (9) David, C., Arnou, B., Sanchez, J.-F., Pelosi, L., Brandolin, G., Lauquin, G. J.-M., and Trézéguet, V. (2008) Two residues of a conserved aromatic ladder of the mitochondrial ADP/ATP carrier are crucial to nucleotide transport. *Biochemistry* 47, 13223–13231.
- (10) Sanchez, J.-F., Kauffmann, B., Grélaud, A., Sanchez, C., Trézéguet, V., Huc, I., and Lauquin, G. J.-M. (2012) Unambiguous structure of atractyloside and carboxyatractyloside. *Bioorg. Med. Chem. Lett.* 22, 2973–2975.
- (11) Brandolin, G., Meyer, C., Dalbon, P., Vignais, P. M., and Vignais, P. V. (1974) Partial purification of an atractyloside-binding protein from mitochondria. *FEBS Lett.* 46, 149–153.
- (12) Block, M. R., Lauquin, G. J.-M., and Vignais, P. V. (1982) Interaction of 3'-O-(1-naphthoyl)adenosine 5'-diphosphate, a fluorescent adenosine 5'-diphosphate analogue, with the adenosine 5'-diphosphate/adenosine 5'-triphosphate carrier protein in the mitochondrial membrane. *Biochemistry* 21, 5451–5457.
- (13) De Marcos Lousa, C., Trézéguet, V., Dianoux, A.-C., Brandolin, G., and Lauquin, G. J.-M. (2002) The human mitochondrial ADP/ATP carriers: Kinetic properties and biogenesis of wild-type and mutant proteins in the yeast *S. cerevisiae*. *Biochemistry* 41, 14412–14420.
- (14) Kushnirov, V. V. (2000) Rapid and reliable protein extraction from yeast. *Yeast* 16, 857–860.
- (15) Woods, A., Sherwin, T., Sasse, R., MacRae, T. H., Baines, A. J., and Gull, K. (1989) Definition of individual components within the cytoskeleton of *Trypanosoma brucei* by a library of monoclonal antibodies. *J. Cell Sci.* 93, 491–500.

- (16) Babot, M., Blancard, C., Lauquin, G. J.-M., and Trézéguet, V. (2012) The transmembrane prolines of the mitochondrial ADP/ATP carrier are involved in nucleotide binding and transport its and biogenesis. *J. Biol. Chem.* 287, 10368–10378.
- (17) Fiore, C., Trézéguet, V., Roux, P., Le Saux, A., Noel, F., Schwimmer, C., Arlot, D., Dianoux, A. C., Lauquin, G. J.-M., and Brandolin, G. (2000) Purification of Histidine-Tagged Mitochondrial ADP/ATP Carrier: Influence of the Conformational States of the C-Terminal Region. *Protein Expression Purif.* 19, 57–65.
- (18) Michejda, J., Guo, X. J., and Lauquin, G. J.-M. (1989) The respiration of cells and mitochondria of porin deficient yeast mutants is coupled. In *Anion Carriers of Mitochondrial Membranes* (Azzi, A., Ed.) pp 225–235, Springer-Verlag, Berlin.
- (19) Arnou, B., Dahout-Gonzalez, C., Pelosi, L., Lauquin, G. J.-M., Brandolin, G., and Trézéguet, V. (2010) Native membrane proteins vs. yeast recombinant: An example: The mitochondrial ADP/ATP carrier. *Methods Mol. Biol.* 654, 19–20.
- (20) Arnold, K., Bordoli, L., Kopp, J., and Schwede, T. (2006) The SWISS-MODEL Workspace: A web-based environment for protein structure homology modelling. *Bioinformatics* 22, 195–201.
- (21) Adams, P. D., Afonine, P. V., Bunkóczi, G., Chen, V. B., Davis, I. W., Echols, N., Headd, J. J., Hung, L. W., Kapral, G. J., Grosse-Kunstleve, R. W., McCoy, A. J., Moriarty, N. W., Oeffner, R., Read, R. J., Richardson, D. C., Richardson, J. S., Terwilliger, T. C., and Zwart, P. H. (2010) PHENIX: A comprehensive Python-based system for macromolecular structure solution. *Acta Crystallogr. D* 66, 213–221.
- (22) Boulay, F., and Vignais, P. V. (1984) Localization of the N-ethylmaleimide reactive cysteine in the beef heart mitochondrial ADP/ATP carrier protein. *Biochemistry* 23, 4807–4812.
- (23) Marty, I., Brandolin, G., Gagnon, J., Brasseur, R., and Vignais, P. V. (1992) Topography of the membrane-bound ADP/ATP carrier assessed by enzymatic proteolysis. *Biochemistry* 31, 4058–4065.
- (24) Vignais, P. V., and Vignais, P. M. (1972) Effect of SH reagents on atractyloside binding to mitochondria and ADP translocation. Potentiation by ADP and its prevention by uncoupler FCCP. *FEBS Lett.* 26, 27–31.
- (25) Lauquin, G. J.-M., and Vignais, P. V. (1976) Interaction of [³H]bongkreic acid with the mitochondrial adenine nucleotide translocator. *Biochemistry* 15, 2316–2322.
- (26) Nury, H., Dahout-Gonzalez, C., Trézéguet, V., Lauquin, G. J.-M., Brandolin, G., and Pebay-Peyroula, E. (2006) Relations between structure and function of the mitochondrial ADP/ATP carrier. *Annu. Rev. Biochem.* 75, 713–741.
- (27) Hoffmann, B., Stöckl, A., Schlame, M., Beyer, K., and Klingenberg, M. (1994) The reconstituted ADP/ATP carrier activity has an absolute requirement for cardiolipin as shown in cysteine mutants. *J. Biol. Chem.* 269, 1940–1944.
- (28) Hatanaka, T., Kihira, Y., Shinohara, Y., Majima, E., and Terada, H. (2001) Characterization of loops of the yeast mitochondrial ADP/ATP carrier facing the cytosol by site-directed mutagenesis. *Biochem. Biophys. Res. Commun.* 286, 936–942.
- (29) Block, M. R., Lauquin, G. J., and Vignais, P. V. (1983) Use of 3'-O-naphthoyladenine 5'-diphosphate to probe distinct conformational states of membrane-bound adenosine 5'-diphosphate/adenosine 5'-triphosphate carrier. *Biochemistry* 22, 2202–2208.
- (30) Zeman, I., Schwimmer, C., Postis, V., Brandolin, G., David, C., Trézéguet, V., and Lauquin, G. J.-M. (2003) Four mutations in transmembrane domains of the mitochondrial ADP/ATP carrier increase resistance to bongkreic acid. *J. Bioenerg. Biomembr.* 35, 243–256.
- (31) Klingenberg, M., Appel, M., Babel, W., and Aquila, H. (1983) The binding of bongkreic acid to mitochondria. *Eur. J. Biochem.* 131, 647–654.
- (32) Wang, Y., and Tajkhorshid, E. (2008) Electrostatic funneling of substrate in mitochondrial inner membrane carriers. *Proc. Natl. Acad. Sci. U.S.A.* 105, 9598–9603.
- (33) Cléménçon, B., Rey, M., Trézéguet, V., Forest, E., and Pelosi, L. (2011) Yeast ADP/ATP carrier isoform 2: Conformational dynamics and role of the RRRMMM signature sequence methionines. *J. Biol. Chem.* 286, 36119–36131.
- (34) Nelson, D. R., and Douglas, M. G. (1993) Function-based mapping of the yeast mitochondrial ADP/ATP translocator by selection for second site revertants. *J. Mol. Biol.* 230, 1171–1182.
- (35) Postis, V., De Marcos Lousa, C., Arnou, B., Lauquin, G. J.-M., and Trézéguet, V. (2005) Subunits of the yeast mitochondrial ADP/ATP carrier: Cooperation within the dimer. *Biochemistry* 44, 14732–14740.
- (36) Dehez, F., Pebay-Peyroula, E., and Chipot, C. (2008) Binding of ADP in the mitochondrial ADP/ATP carrier is driven by an electrostatic funnel. *J. Am. Chem. Soc.* 130, 12725–12733.
- (37) Kihira, Y., Iwahashi, A., Majima, E., Terada, H., and Shinohara, Y. (2004) Twisting of the second transmembrane α -helix of the mitochondrial ADP/ATP carrier during the transition between two carrier conformational states. *Biochemistry* 43, 15204–15209.
- (38) Rey, M., Man, P., Cléménçon, B., Trézéguet, V., Brandolin, G., Forest, E., and Pelosi, L. (2010) Conformational dynamics of the bovine mitochondrial ADP/ATP carrier isoform 1 revealed by hydrogen/deuterium exchange coupled to mass spectrometry. *J. Biol. Chem.* 285, 34981–34990.
- (39) Kihira, Y., Hashimoto, M., Shinohara, Y., Majima, E., and Terada, H. (2006) Roles of adjoining Asp and Cys residues of first matrix-facing loop in transport activity of yeast and bovine mitochondrial ADP/ATP carriers. *J. Biochem.* 139, 575–582.
- (40) Claypool, S. M. (2009) Cardiolipin, a critical determinant of mitochondrial carrier protein assembly and function. *Biochim. Biophys. Acta* 1788, 2059–2068.

■ NOTE ADDED AFTER ASAP PUBLICATION

This paper was published to the Web on September 4, 2012, with a mistake in the author list. This was corrected when the paper was published to the Web on September 18, 2012.